Volume 57(10): 951–962, 2009
Journal of Histochemistry & Cytochemistry
http://www.jhc.org

ARTICLE

Spatiotemporal Organization of AT- and GC-rich DNA and Their Association With Transition Proteins TP1 and TP2 in Rat Condensing Spermatids

Ullas Kolthur-Seetharam,[1] Madapura M. Pradeepa,[1] Nikhil Gupta, Rammohan Narayanaswamy, and Manchanahalli R. Satyanarayana Rao

Department of Biochemistry, Indian Institute of Science, Bangalore, India (UK-S,RN,MRSR), and Jawaharlal Nehru Centre for Advanced Scientific Research, Jakkur, Bangalore, India (MMP,NG,MRSR)

SUMMARY Transition protein 1 (TP1) and TP2 replace histones during midspermiogenesis (stages 12–15) and are finally replaced by protamines. TPs play a predominant role in DNA condensation and chromatin remodeling during mammalian spermiogenesis. TP2 is a zinc metalloprotein with two novel zinc finger modules that condenses DNA in vitro in a GC-preference manner. TP2 also localizes to the nucleolus in transfected HeLa and Cos-7 cells, suggesting a GC-rich preference, even in vivo. We have now studied the localization pattern of TP2 in the rat spermatid nucleus. Colocalization studies using GC-selective DNA-binding dyes chromomycin A3 and 7-amino actinomycin D and an AT-selective dye, 4′,6-diamidino-2-phenylindole, indicate that TP2 is preferentially localized to GC-rich sequences. Interestingly, as spermatids mature, TP2 and GC-rich DNA moves toward the nuclear periphery, and in the late stages of spermatid maturation, TP2 is predominantly localized at the nuclear periphery. Another interesting observation is the mutually exclusive localization of GC- and AT-rich DNA in the elongating and elongated spermatids. A combined immunofluorescence experiment with anti-TP2 and anti-TP1 antibodies revealed several foci of overlapping localization, indicating that TP1 and TP2 may have concerted functional roles during chromatin remodeling in mammalian spermiogenesis. **(J Histochem Cytochem 57:951–962, 2009)**

KEY WORDS
spermiogenesis
DNA-binding dyes
TP1 and TP2
colocalization

THE MAMMALIAN GENOME of $\sim 3–5 \times 10^9$ bp is packaged very tightly inside the sperm nucleus with the help of protamines (protamine P1 and P2 in mice and humans), facilitated by charge neutralization and intermolecular disulfide linkages. In mouse, this packaging results in the sperm nucleus adopting a volume ~40-fold smaller than a normal somatic interphase nucleus (Wyrobek et al. 1976). Although it was originally believed that the entire genome is packaged into nucleoprotamine fibers, more-recent evidence indicates that 2% and 15% of the genome is still associated with histones in mouse and human sperm, respectively (Gatewood et al. 1987,1990). Recently, Nazarov et al. (2008) have demonstrated that chromatin released from human spermatozoa following nuclease digestion exhibits a nucleosomal periodicity of ~195 bp. Specific structural and functional features have been attributed to this nucleohistone fraction, including sequence-specific DNA packaging (Pittoggi et al. 2001) and a role in the regulation of gene expression (Garden et al. 1998). This has been supported by reports showing that parts of the telomeric DNA (Zalenskaya et al. 2000; Li et al. 2008) and retroposon DNA (Pittoggi et al. 1999) are found in the nucleohistone fraction. These unexpected observations and the presence of transcription factors in sperm chromatin (Pittoggi et al. 2001) raise an interesting question as to the nature of the chromatin domains that remain in nucleosomal context and the possible significance of DNA sequences embedded in these domains in early development following fertilization. Histone retention in the mature sperm might have a role in the packaging of early developmental genes as

Correspondence to: Prof. M.R.S. Rao, Jawaharlal Nehru Centre for Advanced Scientific Research, Jakkur, Bangalore 560064, India. E-mail: mrsrao@jncasr.ac.in
[1]These authors contributed equally to this work.
Received for publication December 30, 2008; accepted May 27, 2009 [DOI: 10.1369/jhc.2009.953414].

 0022-1554/09/$3.30

nucleohistone complexes, as against protamine containing highly condensed chromatin domains to facilitate transcription in the early embryo (reviewed in Ooi and Henikoff 2007).

The spatial organization of genes and chromosomes in an interphase nucleus is non-random (Cremer and Cremer 2001; Kumaran et al. 2008). It is generally believed that gene-rich sequences (GC-rich) are positioned in the interior of the nucleus, whereas the gene-poor sequences (AT-rich) are found in the nuclear periphery (Lanctot et al. 2007). Recent observations suggest that this partitioning of gene-rich sequences between the nuclear periphery and the interior is also dynamic in nature (Branco and Pombo 2006). However, data on the organization of DNA sequences in the mammalian sperm are very few. Overall nuclear architecture in the mammalian sperm cell is arranged in an orderly way wherein all centromeres are internally localized, whereas chromosome ends are exposed to the nuclear periphery, suggesting that chromosomes have preferred intranuclear positioning and that this organization is conserved across species (Zalensky and Zalenskaya 2007).

The transformation of the nucleosomal type of chromatin into nucleoprotamine fiber in haploid spermatids is, however, not a direct replacement process in mammals. There is an intermediate stage during spermiogenesis (stages 12–15) in which the nucleosomal histones are replaced by the transition proteins TP1, TP2, and TP4. The biological significance of the evolution of transition protein genes and their physiological roles are not completely understood. Both $TP1^{-/-}$ and $TP2^{-/-}$ knockout mice have been generated that are less fertile than normal mice and show abnormal chromatin condensation (Yu et al. 2000; Zhao et al. 2001). TP1 and TP2 double-knockout mice are, however, sterile, and spermatogenesis is severely impaired, suggesting their important role in spermiogenesis (Zhao et al. 2004b).

Over the last decade, we have been studying the DNA and chromatin-binding properties of TP1 and TP2 in vitro, in the context of their molecular anatomy and domain architecture (reviewed in Pradeepa and Rao 2007). We had earlier shown that TP2 is a zinc metalloprotein (Baskaran and Rao 1991) and condenses DNA with a preference for GC-rich DNA in a zinc-dependent manner (Kundu and Rao 1995). We have also delineated the domain architecture of TP2 and shown it to possess two structural and functional domains (Meetei et al. 2000). The N-terminal two thirds of TP2, upstream of the lone glutamate 86 residue, has two novel zinc finger modules comprising four histidine and four cysteine residues, respectively. The C-terminal one third of TP2 contains the nuclear localization signal and also the basic DNA condensing domain. Our observations showing a preferential localization of TP2 to nucleolus in ectopically expressed HeLa and Cos-7 cells also suggested that TP2 might prefer GC-rich DNA in vivo (Ullas and Rao 2003).

At this juncture, we were curious to examine the nature of DNA sequences associated with TP2 in vivo in elongating spermatids. For this purpose, we have made use of a combination of an immunofluorescence technique using TP1- and TP2-specific antibodies along with the fluorescent DNA-binding GC-selective dyes chromomycin A3 (CMA3) and 7-amino actinomycin D (7-AAD), and AT-selective 4′,6-diamidino-2-phenylindole (DAPI). Results presented in this communication have revealed that there is a spatiotemporal organization of DNA sequences during the elongation of haploid round spermatids and that TP2 colocalizes with GC-rich DNA, providing further in vivo evidence of its preference for GC-rich sequences. Interestingly, several foci were observed wherein both TP1 and TP2 are colocalized, suggesting a possible cooperative role for these two transition proteins in the global chromatin remodeling process during the later stages of spermiogenesis.

Materials and Methods

Sonication-resistant Spermatid (SRS) Nuclei and Western Blot Analysis

SRS nuclei were prepared from total testicular cells as described by Singh and Rao (1987), and 0.4 N HCl soluble proteins of these nuclei, after separation on 12% SDS-PAGE, were probed with anti-TP1 and anti-TP2 monospecific antibody (Sudhakar and Rao 1990) Anti-TP2 antibody was raised in rabbit and subsequently purified by passing through a TP2 (recombinant)-coupled CNBr-activated sepharose 4B column (Amersham Pharmacia Biotech; Little Chalfont, UK) according to the manufacturer's protocol. Anti-TP1 antibody was raised in rabbit against full-length TP1 purified from rat testis and subsequently purified on a TP1-coupled CNBr-activated sepharose column.

Preparation of Testicular Cells

Adult male Wistar rats 60 days old were used for the preparation of testicular cells. The testes were decapsulated, the tissue minced with a pair of scissors, and the seminiferous tubules then digested with collagenase type IV (400 μg/ml; Sigma, St. Louis, MO) in 100 ml of DMEM supplemented with 25 mM HEPES (pH 7.4) and 0.37% sodium bicarbonate for 90 min at room temperature. The released single-cell suspension of testicular cells was obtained after filtering through four layers of cheesecloth that were processed for indirect immunofluorescence analysis. Haploid spermatids containing the round, elongating, and elongated spermatids were further isolated from the total testicular preparation by the centrifugal elutriation technique as described previously (Sudhakar and Rao 1990).

Decondensation of Testicular Cells

Decondensation of testicular cells was done as described by Li et al. (2008) with minor modifications. Briefly, total testicular cells obtained as described above were swollen by resuspending in decondensation buffer containing 0.05 mg/ml heparin (Sigma) and 10 mM dithiothreitol (DTT; Sigma) in phosphate-buffered saline (PBS) and incubated on ice for 40 min. Cells obtained after two washes were processed for indirect immunofluorescence analysis. Mock-decondensed cells (incubated in PBS without DTT and heparin) served as control.

Immunofluorescence and Fluorescent Detection of Specific DNA-binding Dyes

Total testicular cell smears were fixed with 4% paraformaldehyde (Merck & Co., Inc.; Whitehouse Station, NJ) for 15 min, followed by a brief treatment with 50 mM ammonium chloride and permeabilized with 0.1% Triton X-100 (Sigma). Fetal calf serum (1%) in PBS was used for blocking nonspecific sites. Purified rabbit anti-TP2 monospecific antibody was used as the primary antibody (250 ng/μl) and anti-rabbit IgG conjugated to FITC was used as the secondary antibody. The GC-specific dyes CMA3 and 7-AAD, and AT-specific DAPI (all from Sigma) were used at the concentration of 0.5 ng/μl. TP1 localization was examined using anti-TP1 monospecific antibody conjugated to FITC. For colocalization studies, anti-TP2 antibody conjugated with tetramethyl rhodamine iso-thiocyanate (TRITC) was used instead of an indirect immunofluorescence procedure. The cells were incubated with their respective antibodies for 45 min at room temperature in a humidified chamber, and in the dark for fluorescent-labeled antibodies. After incubation, the excess antibodies were washed with PBS containing 0.05% Tween 20. Finally, the cells were incubated with CMA3 or 7-AAD dyes for 10 min, and smears were washed to remove excess dye and incubated with DAPI for 5 min before washing with PBS containing 0.05% Tween 20. DABCO (1%) in 90% glycerol (phosphate-buffered) was used as an antifade. The slides were analyzed by confocal laser scanning microscopy (Leica TCS SP1 and LSM 510 META; Carl Zeiss, Oberkochen, Germany). Preset narrow-range excitation and emission wavelengths were used, and the slides were sequentially scanned to eliminate the cross-talk of chromophores. The signals from DAPI, 7-AAD, FITC, and TRITC naturally gave blue, red, green, and red fluorescence, respectively. The fluorescence pattern for CMA3 was color coded red by the software during the acquisition to create better overlay images with the FITC pattern. The images were analyzed for colocalization parameters using Carl Zeiss LSM software v3.2. Colocalized areas of images were quantified and visualized with the aid of scatter plots and cut-mask function, respectively, as described by the manufacturer. In a scatter plot, pixels from individual channels tend to cluster more toward the axes (quadrants 1 and 2) of the plot; colocalized pixels appear toward the middle (quadrant 3) of the plot. By cross-hair function, only pixels in quadrant 3 of the plot were selected for generating the cut-mask image. We have also quantified the number of colocalized pixels in the images using Manders overlap coefficient (MOC), which is a measure of the overlap of the signals and thus represents the true degree of colocalization. Values of the MOC are defined from 0 to 1.0. A number of 1.0 implies that 100% of both its components overlap with the other part of the image (Manders et al. 1993). Serial Z sections were also taken to confirm colocalization in different planes.

Results

We have shown previously that the transition protein TP2 binds and condenses GC-rich sequences preferentially (Kundu and Rao 1995). Our observation that

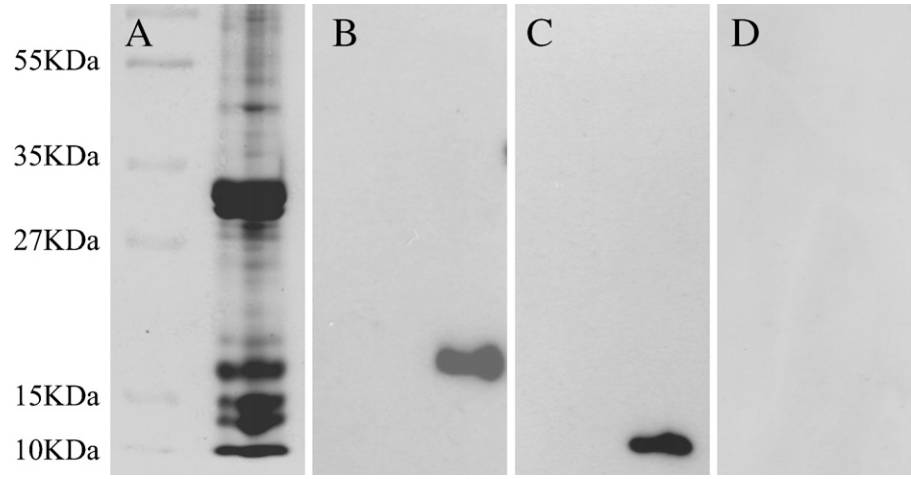

Figure 1 Specificity of transition protein 1 (TP1) and TP2 antibodies: Specificity of antibodies was checked by performing a Western blot with affinity-purified TP2 and TP1 antibodies. **(A)** Protein profile of acid extract from sonication-resistant spermatid nuclei separated on 12% SDS-PAGE and stained with Coomassie Brilliant Blue. **(B)** Western blot with anti-TP2 antibodies. **(C)** Western blot with anti-TP1 antibodies. **(D)** Western blot probed with preimmune sera.

TP2 also localizes to nucleolus in the transfected Cos-7 and HeLa cells (Ullas and Rao 2003) indicated that TP2 prefers GC-rich sequences, even in vivo. These results were, however, obtained in ectopically expressed HeLa and Cos-7 cells, whereas TP2 is expressed only in the testis, in a stage-specific manner. We were curious to examine whether TP2 prefers GC-rich sequences in its natural environment, that is, in elongated spermatids. Toward this goal, we have carried out a detailed investigation to study the localization pattern of TP2 along with GC-rich–binding dyes in elongating spermatids. Several DNA-binding dyes have been used in the literature to study the properties and localization of GC- and AT-rich sequences (Murata et al. 2001). Among these, we have selected CMA3 and 7-AAD as GC-selective and DAPI as AT-selective DNA-binding dyes in the present study. For protein colocalization studies, we have used highly specific anti-TP2 and anti-TP1 antibodies as demonstrated in Figure 1 by Western blot analysis of total acid-soluble proteins of sonication-resistant spermatid nuclei from testicular cells of 60-day-old rats.

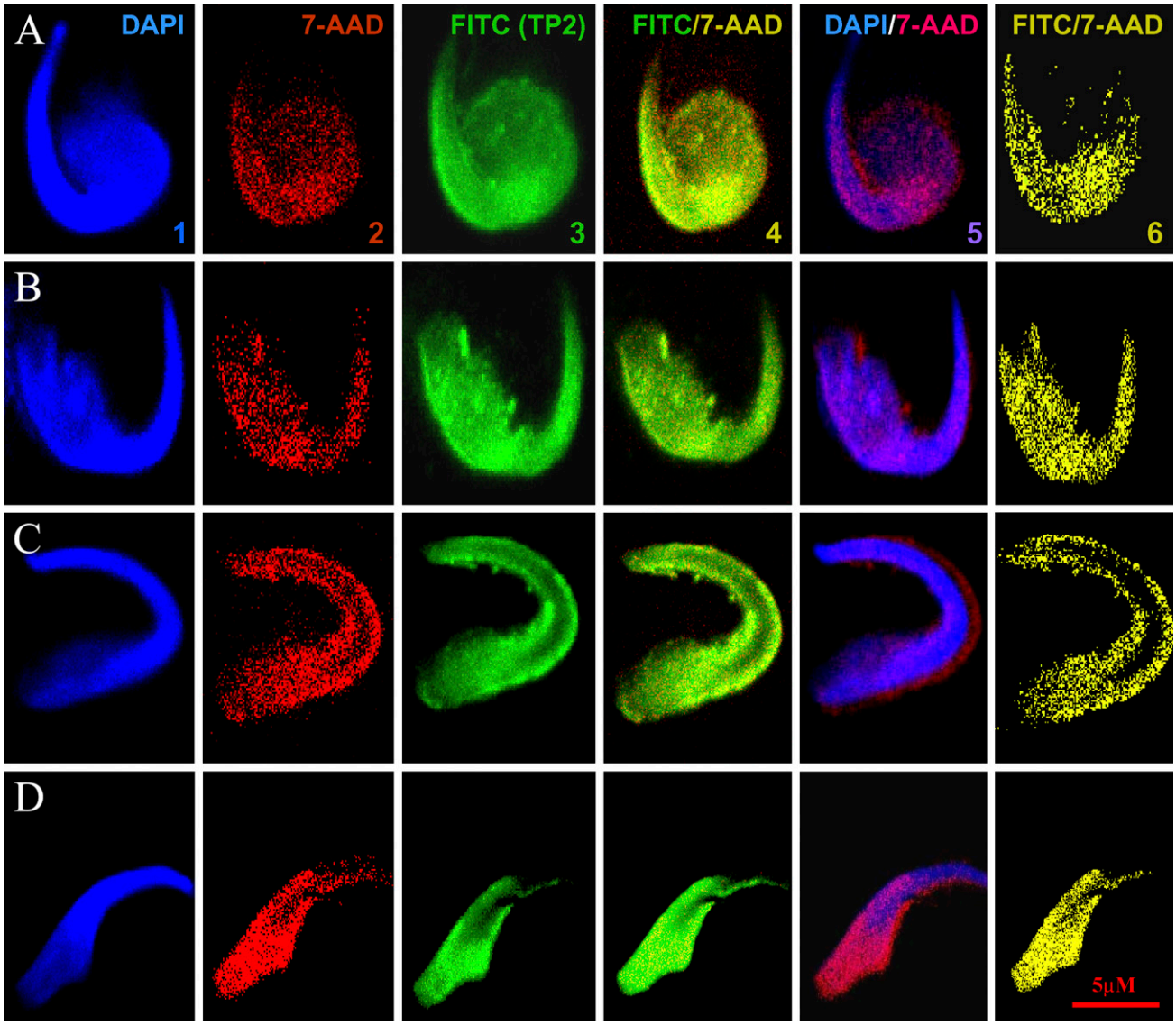

Figure 2 Colocalization of endogenous TP2 and 7-amino actinomycin D (7-AAD) in elongating spermatids. (**A–D**) Spermatids at different stages of maturation. Columns from left to right show fluorescence patterns of 4′,6-diamidino-2-phenylindole (DAPI) (column 1), 7-AAD (column 2), FITC (TP2) (column 3), 7-AAD/FITC (TP2) overlay (column 4), 7-AAD/DAPI overlay (column 5), and 7-AAD/FITC (TP2) overlay (column 6) showing cut-mask images of the colocalized pixels, eliminating background and pixels from individual channels. Columns from left to right show fluorescence patterns of DAPI, FITC, and DAPI/FITC overlay.

The Journal of Histochemistry & Cytochemistry

Colocalization Pattern of TP2 With GC- and AT-binding Dyes

Figure 2 shows the immunofluorescence pattern of TP2 in elongating spermatids at different stages of maturation as visualized by confocal microscopy (Figures 2A–2D). The same smears were probed with both 7-AAD and DAPI and examined under the microscope. As can be seen in column 1, the AT-binding dye is more or less diffusely distributed throughout the nucleus. On the other hand, the GC-rich DNA-binding dye, 7-AAD (Liu et al. 1991), shows a punctate distribution (column 2) suggesting that GC-rich sequences are embedded discretely within the AT-rich mammalian genome. The clear demarcation of the distribution of the AT- and GC-rich DNA within the spermatid nucleus can be much better appreciated in the overlay images of the two dyes shown in column 5. The immunolocalization patterns of TP2 in these stages of spermatids are shown in column 3. It can be seen that in several foci, TP2 shows a very close parallel distribution with the GC-rich DNA-binding dye, 7-AAD. The merged images were obtained for FITC (TP2)/7-AAD (column 4) and DAPI/7-AAD (column 5) using the image acquisition software. A comparison of the fluorescence patterns of TP2 and 7-AAD clearly indicates that in the majority of the foci, they show colocalization, which is evident from the merged image revealing a yellow color (column 4). We also observed that the localization of TP2 and 7-AAD at later stages of spermatid maturation is more concentrated around the periphery of the elongating nucleus and also in the maturing spermatid head (Figures 2C and 2D). It is interesting to note that DAPI fluorescence in these elongating spermatids is more concentrated within the interior of the nucleus. Cut-mask images (generated after removing non-overlapping and background pixels) generated using Zeiss software confirm clear colocalization of TP2 with 7-AAD (column 6) in all stages (Figures 2A–2D). A scatter plot was generated to see the extent of overlapping between TP2 and 7-AAD, which is shown in Figure 3A, whereas Figure 3B represents a software-generated image of the localization pattern of TP2 with 7-AAD. In this scatter plot, pixels in quadrants 1 and 2 represent individual pixels of red and green and the pixels in quadrant 3 represent the colocalized pixels of the image. The number of pixels in quadrant 3 was 14,995, as compared with 4460 pixels in quadrant 1 and 4104 pixels in quadrant 2; thus, the number of overlapping pixels is higher than the two individual foci. The degree of colocalization by numerical colocalization analysis revealed an overlap coefficient of 1.0 in quadrant 3 of Figure 3A. Figure 3C shows the colocalization pattern of TP2 in elongating spermatid nucleus at different planes of the confocal sections. It is clear that the colocalization of TP2 with GC-rich–binding dye is observed at several foci in all sections across the z axis.

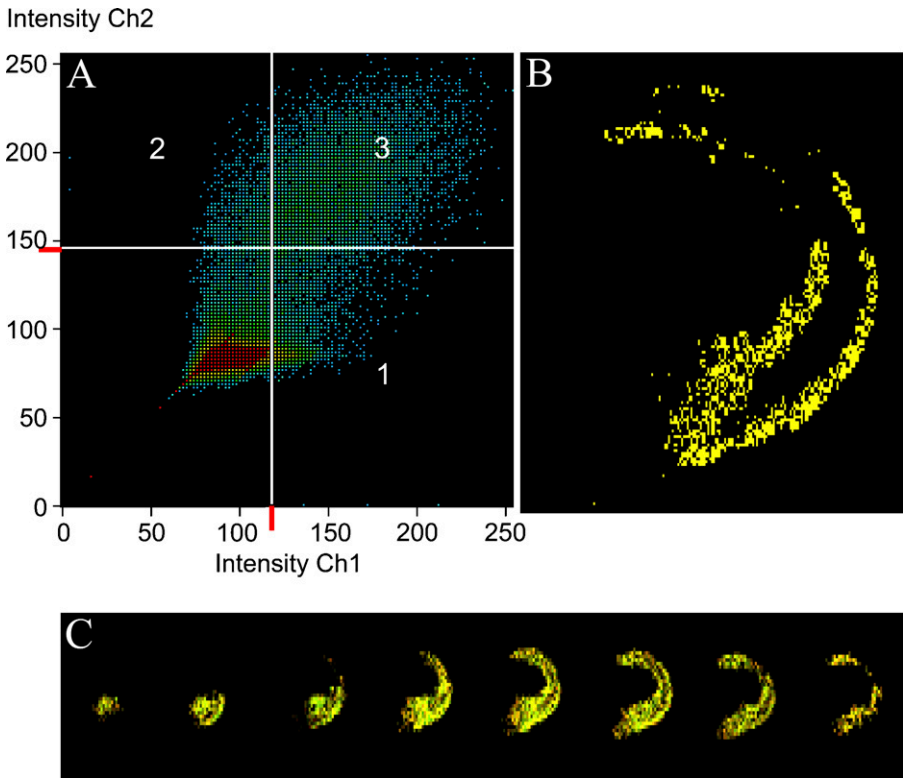

Figure 3 Analysis of colocalized area of TP2 and 7-AAD using Zeiss software. (**A**) Scatter plot showing pixels of TP2 and 7-AAD in the image, where pixels in quadrants 1 and 2 represent pixels of individual green (TP2) and red (7-AAD) channels, whereas the bottom left quadrant shows background pixels, and the pixels in quadrant 3 represent paired pixels (colocalized) of FITC and 7-AAD. (**B**) Cut-mask image showing only colocalized pixels (quadrant 3) in the image, eliminating background and pixels from individual channels. (**C**) Z-stacked images of different planes of spermatids stained with FITC (TP2)/7-AAD.

To further confirm the above observations, we carried out similar studies with another GC-selective DNA-binding drug, CMA3 (Gao and Patel 1989). Figures 4A–4D represent the pattern obtained with elongating spermatids at different stages of maturation. Figures 4A and 4B show early-elongating spermatids; Figures 4C and 4D show late-elongating spermatids; columns 1 to 6 represent the individual fluorescence images and their merged pattern. It is clear that even with CMA3, TP2 shows a colocalization pattern at several foci, as was observed with 7-AAD (Figure 4B, columns 2, 3, and 4). It is interesting to note that CMA3 also shows a mutually exclusive binding pattern with respect to DAPI in the later stages of elongated spermatid (Figure 4C, columns 1, 2, and 5). An important observation that can be noted from Figure 4 that was not convincingly evident in Figure 2 is that at initial stages of spermatid elongation, TP2 and its associated GC-rich sequences are localized to the posterior end of the spermatid nucleus (Figure 4A). In elongating spermatids at later stages of maturation, several discrete foci are observed within the nuclear structure (Figure 4B). Subsequently, they are found near the nuclear periphery (Figure 4C) and finally concentrated at the anterior region of the sickle-shaped spermatid nucleus (Figure 4D). The cut-mask image after colocalization analysis showing only colocalized pixels of CMA3 and TP2 confirms clear colocalization (column 6). The scatter plot of the DNA-binding dye CMA3 and TP2 immunolocalization of selected images

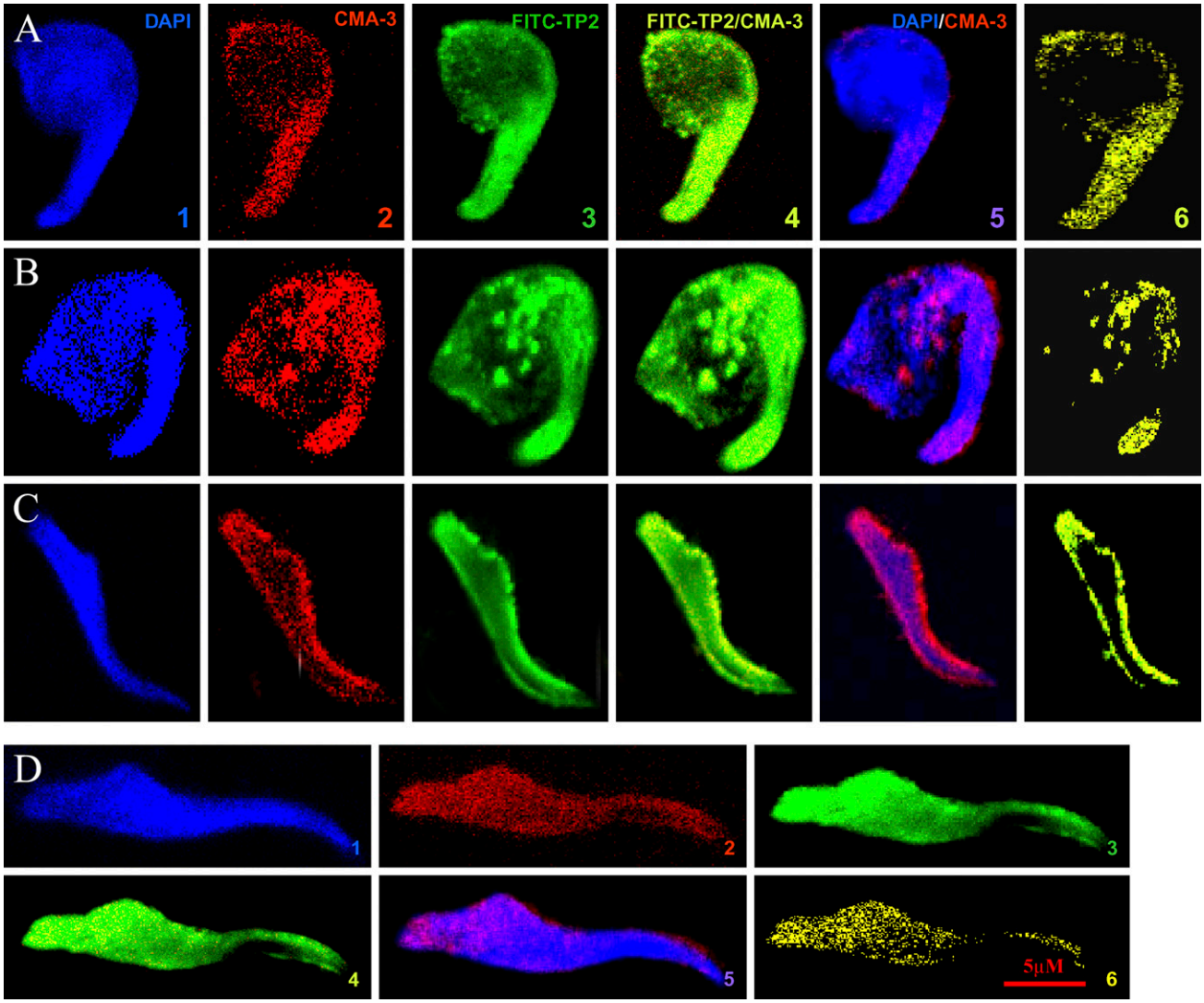

Figure 4 Localization of endogenous TP2 and chromomycin A3 (CMA3) in elongating spermatids. (**A–D**) Spermatids at different stages of maturation. Columns from left to right show fluorescence patterns of DAPI (column 1), CMA3 (column 2), FITC-TP2 (column 3), CMA3/FITC (TP2) overlay (column 4), CMA3/DAPI overlay (column 5), and CMA3/FITC (TP2) overlay (column 6), showing only cut-mask image of the colocalized pixels, eliminating background and individual pixels.

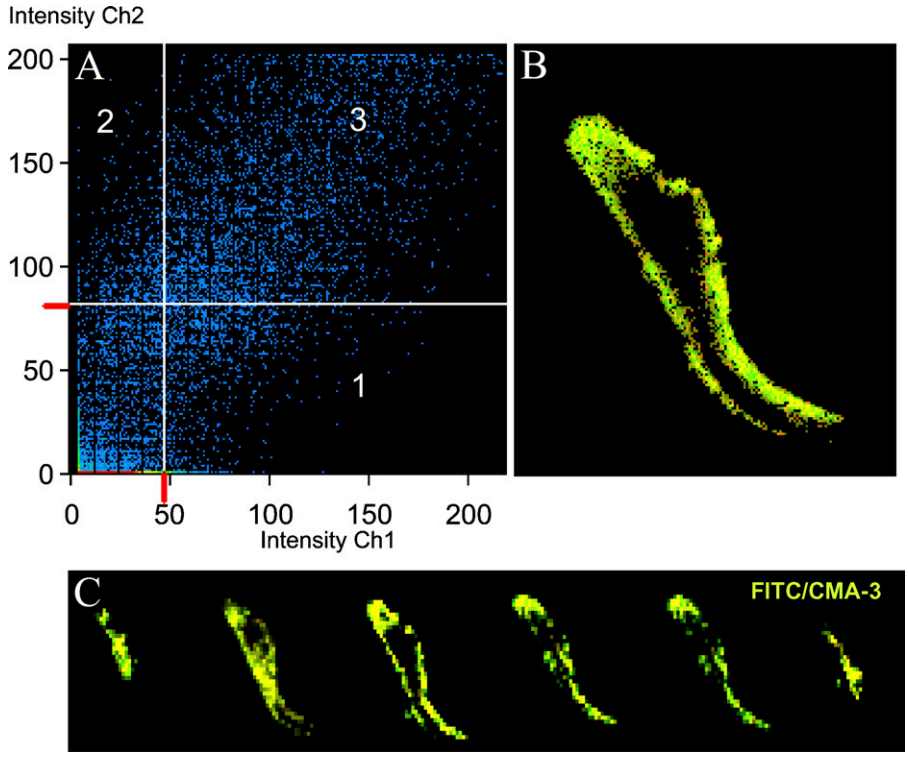

Figure 5 Analysis of colocalized area of TP2 and CMA3 using Zeiss software. (**A**) Scatter plot showing TP2 and CMA3in the image. (**B**) Cut-mask area showing only colocalized pixels in the image. (**C**) Z-stacked images of different planes of spermatids stained with FITC (TP2)/CMA3.

from Figure 4 is shown in Figure 5A. As can be seen, there are several foci in quadrant 3 representing clear overlapping foci of CMA3 and TP2. A software-generated image constituting pixels of quadrant 3 is shown in Figure 5B. The number of pixels in quadrant 3 was 3084 as compared with 733 pixels in quadrant 1 and 735 pixels in quadrant 2. The overlap coefficient was calculated to be 1.0. Again, to be sure that the observed localization pattern does represent a true picture within the nucleus, we have captured the confocal images at multiple planes across the z axis, and the image of one of the spermatid nuclei across the z axis is shown in Figure 4C. These images were obtained with two different GC-rich DNA-binding dyes and therefore provide unequivocal evidence for the association of TP2 with GC-rich sequences in vivo, substantiating our earlier in vitro studies (Kundu and Rao 1995). We would like to add here that the pattern of localization of TP2 and the DNA-binding dyes is observed in most of the spermatid nuclei examined, and only representative images are shown here.

Colocalization Studies on TP1 and TP2

The gene knockout experiments have shown that in both TP1- and TP2-null mice, there is abnormal chromatin condensation (Yu et al. 2000; Zhao et al. 2001). These mice do, however, produce a reduced number of sperm, indicating that spermatogenesis does proceed to completion. This has been interpreted to imply that TP1 and TP2 may have some overlapping and redundant functions in the chromatin remodeling process. A more recent study has, however, shown that the $TP1^{-/-}/TP2^{-/-}$ double-knockout mice are infertile (Zhao et al. 2004b). In this context, we were curious to examine the localization pattern of TP1 and TP2 with respect to each other in the elongating spermatid nucleus using the immunofluorescence technique. For this purpose, anti-TP1 antibodies were tagged with FITC and anti-TP2 antibodies with TRITC. Direct immunofluorescence localization patterns of TP1 and TP2 in elongating spermatids are shown in Figure 6. Figures 6A and 6B show the localization pattern of TP1 within the spermatid nucleus at two different stages of maturation. As observed with TP2, TP1 also showed a preferential localization at the nuclear periphery and at later stages, as specific foci within the sickle-shaped spermatid nucleus. We also observed that anti-TP1 antibodies did not light up spermatids at the earlier stages of maturation in which TP2 was detected (Figures 2 and 3; data not shown). These observations agree with an earlier report (Kistler et al. 1996) showing that TP1 appears later than TP2 during spermiogenesis. Figures 6C and 6D show the coimmunofluorescence pattern of TP1 and TP2. As can be seen in column 4, there are several foci showing colocalization of TP1 and TP2, particularly at the nuclear periphery. This is more apparent in the software-generated cut-mask im-

The Journal of Histochemistry & Cytochemistry

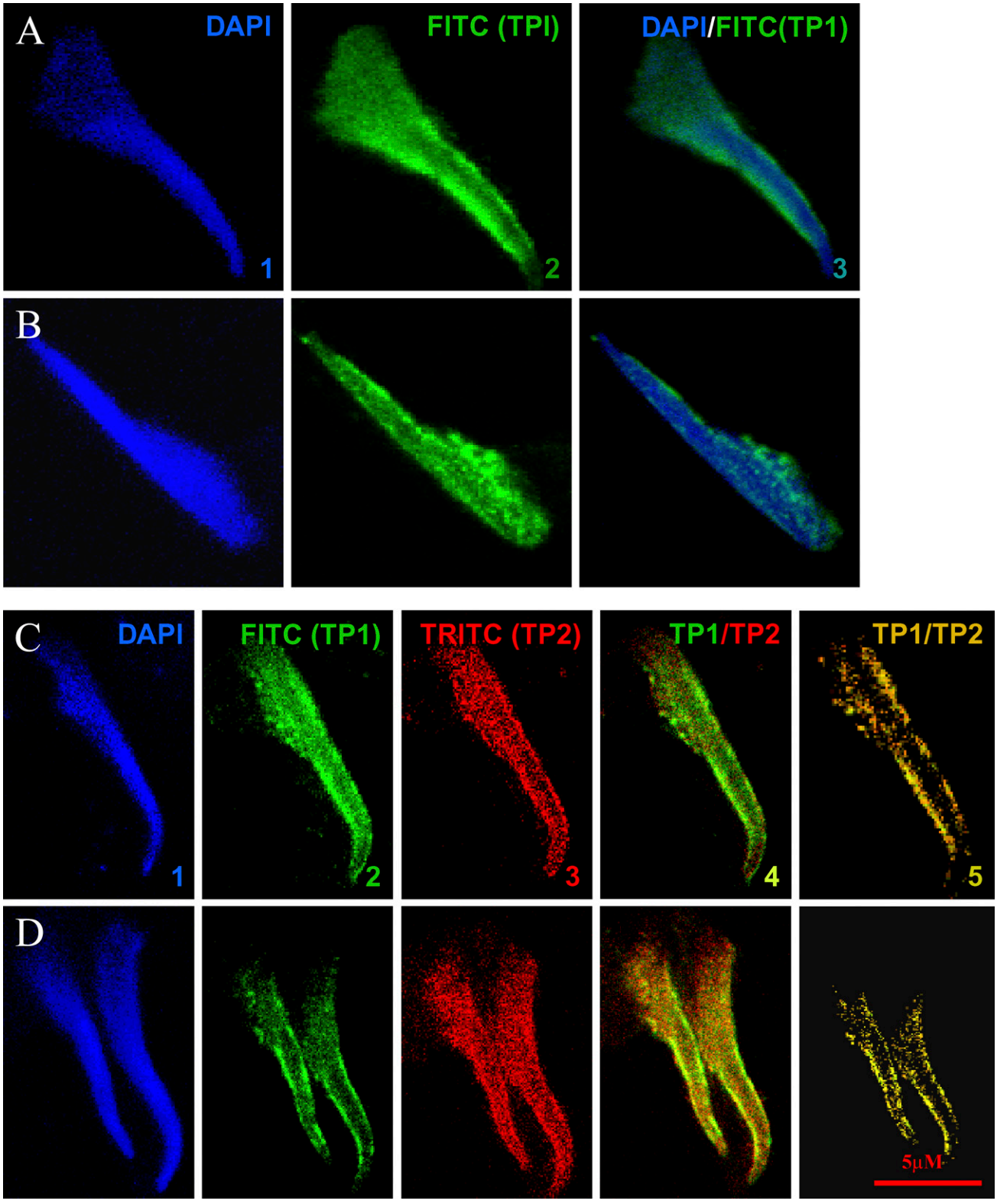

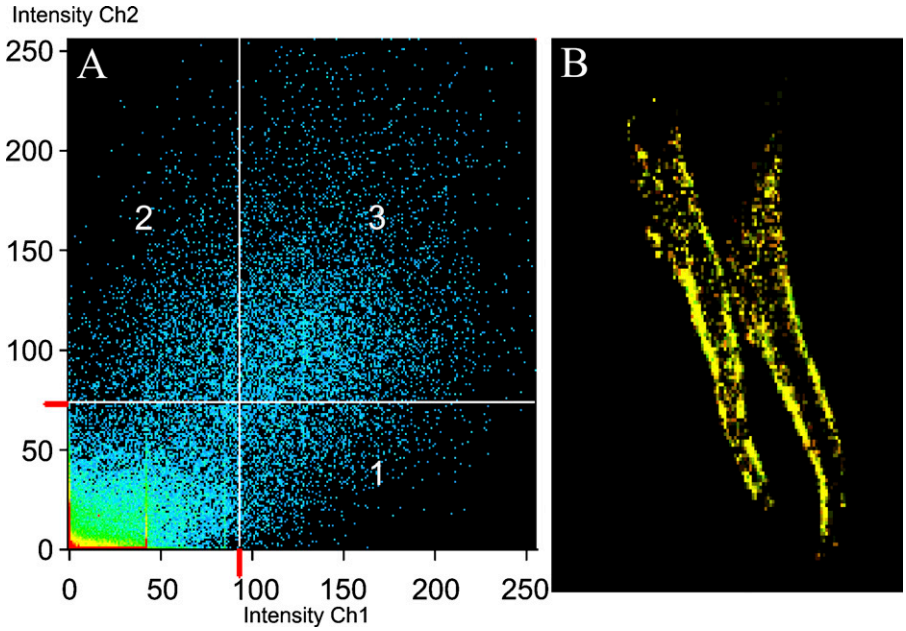

Figure 7 Analysis of colocalized area of TP2 and TP1 using Zeiss software. (**A**) Scatter plot for pixels of TP1 and TP2 in the representative image where pixels in quadrants 1 and 2 represent pixels of individual red (TP2) and green (TP1) channels and the pixels in quadrant 3 represent paired pixels (colocalized) TP2 and TP1. (**B**) Cut-mask area showing only colocalized pixels of TP1 and TP2 in the image.

age of the colocalization pattern (column 5). Figure 7A shows the scatter plot of the fluorescent outputs of TP1 and TP2 localization. Most of the foci are seen in quadrant 3 (12,688 pixels), showing a clear overlapping localization of TP1 and TP2, in addition to many individual foci that are apparent in quadrants 1 (4923 pixels) and 2 (4347 pixels). A representative software-generated cut-mask image confirming overlapping localization of TP1 and TP2 is shown in Figure 7B. Recently, Li et al. (2008) have used a decondensation technique to allow antibody to penetrate in human spermatozoa. We used this technique to examine the overall pattern of TP2 and TP1 localization in the condensing spermatid (Figure 8). Figures 8A and 8C show the mock-decondensed spermatids, covering a few stages of spermiogenesis probed with anti-TP2 and anti-TP1 antibody, respectively. Figures 8B and 8D show the decondensed spermatids covering stages similar to those shown in Figures 8A and 8C. The presence of TP2 and TP1 can be seen in the interior of the nucleus after decondensation, compared with mock-decondensed spermatids.

Discussion

The hallmark of mammalian spermiogenesis is the dramatic chromatin remodeling process wherein the nucleosomal histones are replaced first by the transition proteins TP1, TP2, and TP4 and subsequently by the protamines P1 and P2. In this global remodeling process, a small percentage of the chromatin is retained in the nucleosomal organization, but the significance of nucleosomal chromatin in mature sperm or post-fertilization stages needs to be examined (Nazarov et al. 2008). Much of our understanding of the biological functions of the transition proteins has come from in vitro biochemical and molecular studies of TP1 and TP2 from our laboratory (reviewed in Pradeepa and Rao 2007) and gene knockout studies (Zhao et al. 2004a,b). The present series of experiments was primarily designed to examine the nature of the localization pattern of TP2 in elongating and elongated spermatids with respect to the nature of DNA sequences, particularly in the context of its preference for GC-rich sequences in vitro. We have made use of two GC-rich DNA-binding dyes, 7-AAD and CMA3, in combination with immunofluorescence with monospecific anti-TP2 antibody. The results presented in this article on the immunolocalization pattern of TP2, along with the DNA-binding dyes using confocal microscopy, have given unequivocal evidence that a majority of the TP2 foci colocalize to GC-rich DNA sequences in both elongating and elongated spermatids. Although we had

Figure 6 Localization of endogenous TP1 and TP2 in elongating spermatids. (**A,B**) Localization pattern of TP1 in elongating spermatids at different stages of maturation. Columns from left to right show fluorescence patterns of DAPI (column 1), FITC (TP1) (column 2), and DAPI/FITC (TP1) overlay (column 3), as indicated. (**C,D**) Localization patterns of TP1 and TP2 in elongating spermatids at different stages of maturation. Columns from left to right show fluorescence patterns of DAPI (column 1), FITC (TP1) (column 2), TRITC (TP2) (column 3), FITC (TP1)/TRITC (TP2) (column 4) overlay and cut-mask images of the colocalized pixels of TP1 and TP2 after eliminating background and pixels from individual channels. As indicated, anti-TP1 antibodies were conjugated with FITC, whereas anti-TP2 antibodies were conjugated with TRITC.

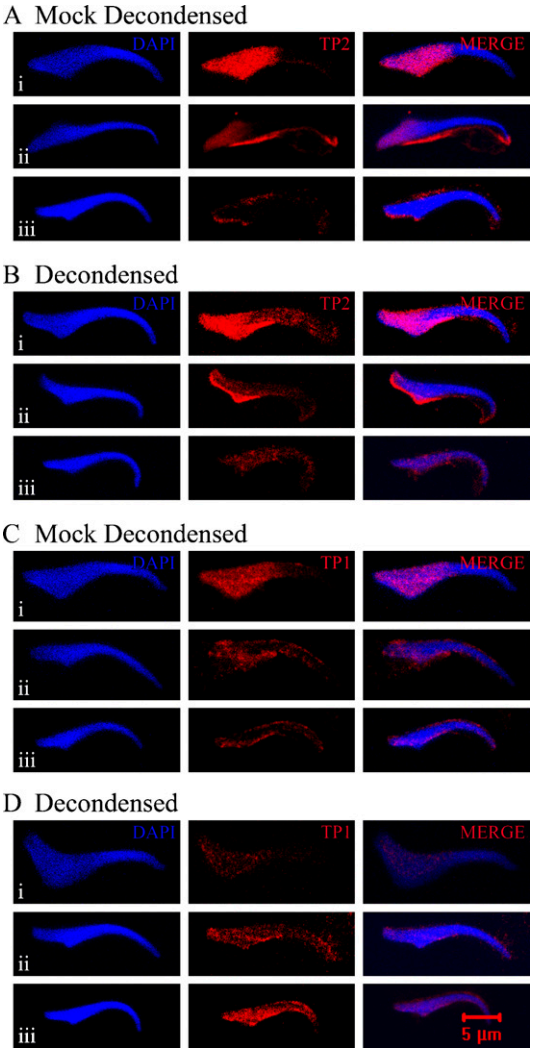

Figure 8 Localization of TP2 and TP1 protein after decondensation of elongating spermatids. Mock-decondensed (**A,C**) and decondensed (**B,D**) spermatid nuclei were probed with TP2/TP1 antibody to study the localization pattern of TP2 (**A,B**) and TP1 (**C,D**) in elongating spermatids at different stages of maturation. Columns from left to right show fluorescence patterns of DAPI, FITC (TP2/TP1), and DAPI/FITC (TP2/TP1) overlay, as indicated.

interpreted the localization of TP2 to the nucleolus in our previous study (Ullas and Rao 2003) as an indicator of the preference for GC-rich sequences, we were concerned about the physiological relevance of such an observation, because there is no defined nucleolar structure in haploid spermatids (Ullas and Rao 2003). In this context, the present results clearly provide unequivocal evidence for the preferential localization to GC-rich sequences of TP2 in its natural context. It should also be mentioned here that there are several foci in both the elongating and elongated spermatids that do not show overlap of TP2 and the GC-rich DNA-binding dyes (as seen in the scatter plot). It is quite possible that the overlapping foci may represent regions of the genome in which there are multiple CpG dinucleotide sequences, such as the CpG islands, and hence TP2 may be more concentrated. In fact, we had shown earlier that TP2 binds to a human CpG island sequence preferentially in vitro in a zinc-dependent manner (Kundu and Rao 1996). A recent report by Foster et al. (2005) has shown that CpG island–containing R bands of porcine chromosomes 2, 3p, 5p, 6, 7, 10, 13, 14, and 17 are preferentially localized to the peripheral and intermediate regions of spermatozoa, with very little present in the sperm interior. It is also worth mentioning here that the vertebrate genome is also made up of different isochors, depending on their GC content (Costantini et al. 2009). Such a spatiotemporal organization of GC- and AT-rich DNA in condensing spermatids may also reflect a similar positioning of isochors also in the mammalian sperm nuclei. It would also be challenging to identify the genomic occupancy sites of TP2 and TP1 in condensing spermatids using the ChIP-on-CHIP technique.

It is becoming increasingly evident that chromosomes are highly organized and compartmentalized into their own specific regions, known as chromosome territories (Cremer and Cremer 2001). Human chromosomes have been found to reproducibly occupy specific nuclear addresses, with an internal nuclear positioning for chromosomes with a high gene density and a more-peripheral position for chromosomes with low gene densities (Habermann et al. 2001). This organization of gene-dense and gene-poor chromosomes is evolutionarily conserved, and several reports show that chromosomes in sperm nuclei are also organized in distinct territories in several species (Tanabe et al. 2002). Although these data seem to suggest that spatial organization of chromosome territory in the sperm nucleus might be different from that in the interphase nucleus (Cremer and Cremer 2001), a detailed comparative study using chromosome-painting probes is warranted. Such a study of the spatial organization of different chromosomes during sperm maturation is also important to understand the packaging of chromatin and its accessibility to immediate activation of paternal gene expression following fertilization. In this context, it is interesting to note that a differential nuclear architecture of chromosome/gene territories from that of a somatic nucleus has been observed recently in rod photoreceptor cells (Slovei et al. 2009).

Another noteworthy observation made in the present study is that TP2 and the associated GC-rich DNA seem to be predominantly localized to the apical region or nuclear periphery in the final stages of spermiogenesis. However, TP2 and GC-rich DNA localize throughout the nucleus in the early-elongating spermatids. In the more mature elongated spermatid, they are highly concentrated in the nuclear head (Figures 2D

and 3D). One of the drawbacks of such an interpretation is the possibility of lack of penetration of the antibody into the core of the nucleus. In fact, after decondensation of these nuclei, we did observe some fluorescence signal for TP2 and TP1 in the interior of the nucleus, although the majority of the fluorescent signal was still localized to the periphery. It is worth mentioning here that Oko et al. (1996) observed TP1 and TP2 in the interior of the condensing spermatids by immunoelectron microscopy. Of more importance, there is not much difference in the localization pattern of TP2 in early-condensing spermatids, as shown in Figure 8A (panel i) and Figure 8B (panel i), showing similar staining for TP2 throughout the nucleus in both the mock-decondensed and decondensed spermatid, respectively. A similar pattern was observed for TP1, as shown in Figure 8C (panel i) and Figure 8D (panel i). In the later stages of condensing spermatids, there was a difference in the localization pattern of TP1 and TP2 between decondensed and mock-decondensed spermatids. Some foci were observed for both TP1 and TP2 in the interior of the nucleus after decondensation (Figures 8A–8D, panels ii and iii). Thus, colocalization of TP2 with GC-rich DNA at the nuclear periphery is not affected, even after decondensation. In this context, a more detailed study of the internal localization pattern of TP2 and TP1 in spermatids of well-defined stages isolated using the technique of Kotaja et al. (2004) will be very valuable and informative.

The results of the immunofluorescence experiment presented in this study show colocalization of TP1 and TP2 in many foci in elongating spermatids, suggesting that they may indeed cooperate with each other in some step(s) relevant for chromatin remodeling during spermiogenesis, in addition to their independent functions. At present, molecular studies have shown clearly that TP1 stimulates DNA repair activity in vitro (Caron et al. 2001), whereas there is strong evidence that TP2 is more closely associated with DNA and consequently the chromatin condensation process (Singh and Rao 1987; Kundu and Rao 1995; Zhao et al. 2004a,b). In the $TP1^{-/-}$ and $TP2^{-/-}$ single-knockout mice, the chromatin condensation process is severely hampered, but still produces some sperm that are capable of fertilization (Shirley et al. 2004). One of the interpretations given for only a subtle effect of the lack of individual transition proteins TP1 and TP2 in single-knockout mice is that the two transition proteins may have overlapping and redundant functions and the lack of one is compensated for by the other (Yu et al. 2000; Zhao et al. 2001). It is hard to imagine such an overlapping function between TP1 and TP2, particularly because the amino acid sequences of the two proteins are very different, with no common functional motifs between them, except for the presence of long stretches of basic amino acids. A more-defined in vitro remodeling assay will be very valuable in unraveling the molecular mechanisms involved in the nucleoprotein transition that takes place in the final steps of mammalian spermiogenesis.

Literature Cited

Baskaran R, Rao MR (1991) Mammalian spermatid specific protein TP2 is a zinc metalloprotein with two finger motifs. Biochem Biophys Res Commun 179:1491–1499

Branco MR, Pombo A (2006) Intermingling of chromosome territories in interphase suggests role in translocations and transcription-dependent associations. PLoS Biol 4:e138. Published online April 25, 2006 (DOI: 10.1371/journal.pbio.0040138)

Caron N, Veilleux S, Boissonneault G (2001) Stimulation of DNA repair by the spermatidal TP1 protein. Mol Reprod Dev 58: 437–443

Costantini M, Cammarano R, Bernardi G. (2009) The evolution of isochore patterns in vertebrate genomes. BMC Genomics 10:146

Cremer T, Cremer C (2001) Chromosome territories, nuclear architecture and gene regulation in mammalian cells. Nat Rev Genet 2:292–301

Foster HA, Abeydeera LR, Griffin DK, Bridger JM (2005) Non-random chromosome positioning in mammalian sperm nuclei, with migration of the sex chromosomes during late spermatogenesis. J Cell Sci 118:1811–1820

Gao X, Patel DJ (1989) Solution structure of the chromomycin-DNA complex. Biochemistry 28:751–762

Garden GM, Ballesteros M, Gordon M, Tam PP (1998) Histone- and protamine-DNA association: conservation of different patterns within the beta-globin domain in human sperm. Mol Cell Biol 18:3350–3356

Gatewood JM, Cook GR, Balhorn R, Bradury EM, Schmid CW (1987) Sequence-specific packaging of DNA in human sperm chromatin. Science 236:962–964

Gatewood JM, Cook GR, Balhorn R, Schmid CW, Bradury EM (1990) Isolation of four core histones from human sperm chromatin representing a minor subset of somatin histones. J Biol Chem 265:20662–20666

Habermann FA, Cremer M, Walter J, Kreth G, von Hase J, Bauer K, Wienberg J, et al. (2001) Arrangements of macro- and microchromosomes in chicken cells. Chromosome Res 9:569–584

Kistler WS, Henriksen K, Mali P, Parvinen M (1996) Sequential expression of nucleoproteins during rat spermiogenesis. Exp Cell Res 225:374–381

Kotaja N, Kimmins S, Brancorsini S, Hentsch D, Vonesch JL, Davidson I, Parvinen M, et al. (2004) Preparation, isolation and characterization of stage-specific spermatogenic cells for cellular and molecular analysis. Nat Methods 1:249–254

Kumaran RI, Thakar R, Spector DL (2008) Chromatin dynamics and gene positioning. Cell 132:929–934

Kundu TK, Rao MR (1995) DNA condensation by the rat spermatidal protein TP2 shows GC-rich sequence preference and is zinc dependent. Biochemistry 34:5143–5150

Kundu TK, Rao MR (1996) Zinc dependent recognition of human CpG island sequence by mammalian spermatidal protein TP2. Biochemistry 35:15626–15632

Lanctot C, Cheuitin T, Cremer M, Cavalli G, Cremer T (2007) Dynamic genome architecture in the nuclear space: regulation of gene expression in three dimensions. Nat Rev Genet 8:104–115

Li Y, Lalancette C, Miller D, Krawetz SA (2008) Characterization of nucleohistone and nucleoprotamine components in the mature human sperm nucleus. Asian J Androl 10:535–541

Liu X, Chen H, Patel DJ (1991) Solution structure of actinomycin-DNA complexes: drug intercalation at isolated G-C sites. J Biomol NMR 1:323–347

Manders EMM, Verbeek FJ, Aten AJ (1993) Measurement of colocalization of objects in dual color confocal images. J Microsc 159: 375–382

Meetei AR, Ullas KS, Rao MR (2000) Identification of two novel zinc finger modules and nuclear localization signal in rat sperma-

tidal protein TP2 by site-directed mutagenesis. J Biol Chem 275:38500–38507

Murata S, Herman P, Lakowicz JR (2001) Texture analysis of fluorescence lifetime images of AT- and GC-rich regions in nuclei. J Histochem Cytochem 49:1443–1451

Nazarov IB, Shlyakhtenko LS, Lyubchenko YL, Zalenskaya IA, Zalensky AO (2008) Sperm chromatin released by nucleases. Syst Biol Reprod Med 54:37–46

Oko RJ, Jando V, Wagner CL, Kistler WS, Hermo LS (1996) Chromatin reorganization in rat spermatids during disappearance of testis-specific histone, H1t, and the appearance of transition proteins TP1 and TP2. Biol Reprod 54:1141–1157

Ooi SL, Henikoff S (2007) Germline histone dynamics and epigenetics. Curr Opin Cell Biol 19:257–265

Pittoggi C, Magnano AR, Sciamanna I, Giordano R, Lorenzini R, Spadafora C (2001) Specific localization of transcription factors in the chromatin of mouse mature spermatozoa. Mol Reprod Dev 60:97–106

Pittoggi C, Renzi L, Zaccagnini G, Cimini D, Degrassi F, Giordano R, Magnano AR, et al. (1999) A fraction of mouse sperm chromatin is organized in nucleosomal hypersensitive domains enriched in retroposon DNA. J Cell Sci 112:3537–3548

Pradeepa MM, Rao MR (2007) Chromatin remodeling during mammalian spermatogenesis: role of testis specific histone variants and transition proteins. Soc Reprod Fertil Suppl 63:1–10

Shirley CR, Hayashi S, Mounsey S, Yanagimachi R, Meistrich ML (2004) Abnormalities and reduced reproductive potential of sperm from Tnp1 and Tnp2-null double mutant mice. Biol Reprod 71: 1220–1229

Singh J, Rao MR (1987) Interaction of rat testis protein, TP, with nucleic acids in vitro. Fluorescence quenching, UV absorption, and thermal denaturation studies. J Biol Chem 262:734–740

Slovei I, Kreysing M, Lanctot C, Kosem S, Peichl L, Cremer T, Guck J, et al. (2009) Nuclear architecture of rod photoreceptor cells adapts to vision in mammalian evolution. Cell 137:356–368

Sudhakar L, Rao MR (1990) Stage-dependent changes in localization of a germ cell-specific lamin during mammalian spermatogenesis. J Biol Chem 265:22526–22532

Tanabe H, Muller S, Neusser M, von Hase J, Calcagno E, Cremer M, Solovei I, et al. (2002) Evolutionary conservation of chromosome territory arrangements in cell nuclei from higher primates. Proc Natl Acad Sci USA 99:4424–4429

Ullas KS, Rao MR (2003) Phosphorylation of rat spermatidal protein TP2 by sperm-specific protein kinase A and modulation of its transport into the haploid nucleus. J Biol Chem 278: 52673–52680

Wyrobek AJ, Meistrich ML, Furrer R, Bruce WR (1976) Physical characteristics of mouse sperm nuclei. Biophys J 16:811–825

Yu YE, Zhang Y, Unni E, Shirley CR, Deng JM, Russell LD, Weil MM, et al. (2000) Abnormal spermatogenesis and reduced fertility in transition nuclear protein 1-deficient mice. Proc Natl Acad Sci USA 97:4683–4688

Zalenskaya IA, Bradbury EM, Zalensky AO (2000) Chromatin structure of telomere domain in human sperm. Biochem Biophys Res Commun 279:213–218

Zalensky A, Zalenskaya I (2007) Organization of chromosomes in spermatozoa: an additional layer of epigenetic information. Biochem Soc Trans 35:609–611

Zhao M, Shirley CR, Hayashi S, Marcon L, Mohapatra B, Suganama R, Behringer RR, et al. (2004a) Transition nuclear proteins are required for normal chromatin condensation and functional sperm development. Genesis 38:200–213

Zhao M, Shirley CR, Mounsey S, Meistrich ML (2004b) Nucleoprotein transitions during spermiogenesis in mice with transition nuclear protein Tnp1 and Tnp2 mutations. Biol Reprod 71: 1016–1025

Zhao M, Shirley CR, Yu YE, Mohapatra B, Zhang Y, Unni E, Deng JM, et al. (2001) Targeted disruption of the transition protein 2 gene affects sperm chromatin structure and reduces fertility in mice. Mol Cell Biol 21:7243–7255

The Journal of Histochemistry & Cytochemistry